PERGAMON

International Journal of Multiphase Flow 28 (2002) 1249–1268

International Journal of Multiphase Flow

www.elsevier.com/locate/ijmulflow

Stability of stratified gas–liquid flows

C. Mata [a], E. Pereyra [a], J.L. Trallero [a], D.D. Joseph [b,*]

[a] PDVSA-Intevep Urb. Santa Rosa, Sector El Tambor, Edo. Miranda P.O. Box 76343, Caracas 1070-A, Venezuela
[b] Department of Aerospace Engineering and Mechanics, University of Minnesota, AEM, 107 Akerman Hall, 110 Union Street, Minneapolis, MN 55455, USA

Received 3 July 2001; received in revised form 1 May 2002

Abstract

We have computed stability limits for Kelvin–Helmholtz instability of superposed gas–liquid flow, comparing theories of others. The theories are compared with literature data on air–water flow and with new data from a 0.0508 m i.d. flow loop at PDSVA-Intevep, using a 0.480 Pa s oil and air.

Keywords: Kelvin–Helmholtz instability; Gas–liquid flow; Bifurcation

1. Introduction

In this paper we compute and compare results from different theories of the Kelvin–Helmholtz (KH) instability of stratified gas–liquid flow with each other, to old data for water–air, and to new data, presented here on heavy oil (0.480 Pa s). The paper is organized as a survey, not done before, but it contains many new results. The theories discussed here are due to Jeffreys (1925, 1926), Taitel and Dukler (1976), Lin and Hanratty (1986), Barnea and Taitel (1993) and Funada and Joseph (2001). The theories make different assumptions and the predicted stability limits differ widely. The identification and comparison of theoretical assumptions with each other and with experiments forms a better basis for evaluating theories than was previously available.

The new data on gas–heavy oil transitions taken in our 0.0508 m i.d. flow loop at PDVSA-Intevep using 0.480 Pa s oil and air addresses problems of production which arise in pumping gas and heavy oil. To select pipes, pumps, motors, etc. for heavy oil reservoirs, traditional correlations of pressure gradient are used. These correlations were developed using fluids with viscosities

* Corresponding author. Tel.: +1-612-626-8000; fax: +1-612-626-1558.
E-mail address: joseph@aem.umn.edu (D.D. Joseph).

0301-9322/02/$ - see front matter © 2002 Published by Elsevier Science Ltd.
PII: S0301-9322(02)00034-4

ranging from 0.001 to 0.005 Pa s. Nevertheless, even for these low viscosity liquids, errors in pressure gradient calculations can be between 20% (Chokshi et al., 1996) and 30 (Gómez et al., 1999). These errors will be greater in the case of extra-heavy oils with viscosities up to 3 Pa s.

To understand gas–liquid flows, flow regimes are very important; slug flow is the predominant flow type for gas–heavy oil flow. Many authors seek to determine the transition to slug flow as a KH instability of stratified flow. In fact, ripples and capillary waves can arise from this instability and the origin of slugs may, in some cases, be associated with a nonlinear transition arising as a subcritical bifurcation as in the case of "premature slugging" observed by Wallis and Dobson (1973).

In our discussion of the linear theories we looked at effects of long waves, short waves and waves of maximum growth, calling attention to the importance of surface tension, which is often incorrectly calculated, evaluated or unjustifiably neglected. The effects of normal stresses and shear stresses are separately evaluated and the consequences of approximating shear stresses and interfacial stresses using correlations are discussed.

The presentation of experimental results, which is usually carried out in the Mandhane plane of superficial gas and liquid velocities, can be misleading because important effects of gas holdups, calculated for data presented here, are ignored.

2. Kelvin–Helmholtz instability

The instability of uniform flow of incompressible inviscid fluids in two horizontal parallel infinite streams of different velocities and densities, one stream above, is better known as the KH instability. It is usual to study this instability by linearizing the nonlinear equations around the basic equations followed by analysis of normal modes proportional to

$$\exp[\sigma t + \mathrm{i}kz] \tag{1}$$

where $\sigma = \sigma_r + \mathrm{i}\sigma_i$ and σ_r is the growth rate, k is the wave number. It is also usual to assume that the fluids are inviscid; if they were viscous the discontinuity of velocity could not persist. Moreover, if the basic streams are assumed uniform then there are no rigorous ways to evaluate the shear and interfacial stresses. In practice, the streams being modeled are turbulent and analytic studies of stability must make approximations. The usual procedure adopted by many authors whose work is reviewed later is to employ empirical correlations for evaluation of shear and interfacial stress. The agreement with experiments achieved by this empirical approach is not compelling.

Funada and Joseph (2001), hereafter called FJ, introduced a new approach to the viscous problem using the theory of viscous potential flow (VPF). This theory allows one to account for the effects of viscosity on extensional stresses activated by the normal displacement of waves while ignoring shear stresses. No assumptions beyond those required for potential flow are invoked.

It is well known that the Navier–Stokes equations are satisfied by potential flow; the viscous term is identically zero when the vorticity is zero but the viscous stresses are not zero (Joseph and Liao, 1994). It is not possible to satisfy the no-slip condition at a solid boundary or the continuity of the tangential component of velocity and shear stress at a fluid-fluid boundary when the velocity is given by a potential. The viscous stresses enter into the VPF analysis of free surface

problems through the normal stress balance at the interface. VPF analysis gives good approximations to fully viscous flows in cases where the shears from the gas flow are negligible; the Rayleigh–Plesset bubble is a potential flow which satisfies the Navier–Stokes equations and all the interface conditions. Joseph et al. (1999) constructed a VPF analysis of the Rayleigh–Taylor instability which can scarcely be distinguished from the exact fully viscous analysis.

The analysis of KH instability using VPF leads to the following dispersion relation:

$$[\rho_G(\sigma + ikU_G)^2 + 2\mu_G k^2(\sigma + ikU_G)]\coth(kh_G) + [\rho_L(\sigma + ikU_L)^2 + 2\mu_L k^2(\sigma + ikU_L)] \times \coth(kh_L) + (\rho_L - \rho_G)gk + \gamma k^3 = 0 \quad (2)$$

where U, h, μ and ρ denote the mean velocity, holdup, viscosity and density respectively. The subscripts G and L stand for gas and liquid. Gravity and surface tension are denoted by g and γ, respectively.

Neutral curves which define the border between stability and instability are the locus of values for which $\sigma_r = 0$; the resulting equation may be solved for

$$V^2(k) = \frac{[\mu_L \coth(kh_L) + \mu_G \coth(kh_G)]^2}{\rho_L \mu_G^2 \coth(kh_L)\coth^2(kh_G) + \rho_G \mu_L^2 \coth^2(kh_L)\coth(kh_G)} \frac{1}{k}[(\rho_L - \rho_G)g + \gamma k^2] \quad (3)$$

where $V = U_G - U_L$ is the relative velocity.

The lowest point on the neutral curve $V^2(k)$ is

$$V_c^2 = \min_{k \geqslant 0} V^2(k) \equiv V^2(k_c), \quad (4)$$

where $\lambda_c = 2\pi/k_c$ is the wave length that makes V^2 minimum. The flow is unstable when

$$V^2 = (-V)^2 > V_c^2.$$

This criterion is symmetric with respect to V and $-V$, depending only on the absolute value of the difference. This feature stems from Galilean invariance; the flow seen by the observer moving with gas is the same as the one seen by an observer moving with the liquid.

The classical theory of KH instability of an inviscid fluid may be obtained from (2) by putting $\mu_G = \mu_L = 0$. In this case (3) reduces to

$$V^2 = \left[\tanh(kh_G) + \frac{\rho_G}{\rho_L}\tanh(kh_L)\right]\left[\frac{g(\rho_L - \rho_G)}{k\rho_G} + \frac{\gamma k}{\rho_G}\right] \quad (5)$$

Most workers, possibly starting with Kordyban and Ranov (1970), have restricted consideration to long waves for which $k \to 0$. This assumption has been employed even by authors who attempt to include viscosity; very important effects of surface tension are lost when $k \to 0$. If $k \to 0$, $\rho_G \ll \rho_L$ and $U_L \ll U_G$, then (5) reduces to

$$U_G^2 = \frac{(\rho_L - \rho_G)}{\rho_G} g h_G,$$

which is the same as

$$j^* = \alpha^{3/2}. \quad (6)$$

Here $\alpha = h_G/H$ and $j^* = U_G \alpha \sqrt{\rho_G}/\sqrt{gH(\rho_L - \rho_G)}$, where H is the channel height.

3. Stability criteria from various authors

The KH linear theory has been used as a basis to determine whether a smooth stratified (SS) flow is stable or not.

Wallis and Dobson (1973) compare their criterion with transition observations that they call "slugging" and note that empirically the stability limit is well described by

$$j^* > 0.5\alpha^{3/2} \tag{7}$$

Taitel and Dukler (1976) (TD) extended the KH analysis first to the case of a finite wave on a flat liquid sheet in horizontal channel flow (8) and then to finite waves on stratified liquid in an inclined pipe (9). In order to apply this criterion they need to provide the equilibrium liquid level h_L (or liquid holdup). They compute h_L through momentum balances in the gas and liquid phases (two fluid model) in which shear stresses are considered and evaluated using conventional friction factors definitions. In the two fluid model, the pipe geometry is taken into account through wetted perimeters by the gas and liquid phases, including the gas–liquid interface. This implies that the wall resistance of the liquid is similar to that for open-channel flow and that of the gas to close-duct flow. This geometry treatment is general and could be applied not only to round pipes, but to any possible shape. With this method, each pair of superficial gas and liquid velocity corresponds to a unique value of h_L. According to TD, a finite wave will grow in a horizontal rectangular channel of height H, when

$$j^* > \left(1 - \frac{h_L}{H}\right)\alpha^{3/2} \tag{8}$$

or

$$U_G > \left(1 - \frac{h_L}{D}\right)\left[\frac{(\rho_L - \rho_G)}{\rho_G}\frac{gA_G}{\frac{dA_L}{dh_L}}\right]^{1/2} \tag{9}$$

for inclined pipe. D is the pipe diameter and A is the cross-section area.

Note that $(1 - h_L/H) = \alpha$. If $h_L/H = 0.5$, $(1 - h_L/H)$ equals 0.5, and this is consistent with the result of Wallis and Dobson (1973).

The TD overall procedure leads to a weak dependence on viscosity, through the calculation of h_L. See Barnea (1991), page 2130.

TD also identify two kinds of stratified flow: stratified smooth (SS) and stratified wavy (SW). These waves, they say, "are caused by the gas flow under conditions where the velocity of the gas is sufficient to cause waves to form, but slower than that needed for the rapid wave growth which causes transition to intermittent or annular flow". TD propose a criterion to predict the transition from SS to SW flow, based on Jeffreys (1925, 1926) ideas.

Jeffreys (1925, 1926) [J] proposed a linear ad hoc theory for the generation of water waves by wind as an alternative to the inviscid KH theory. His argument that the KH theory allows "... no horizontal displacement occurring across the relative velocity of the fluid ..." is erroneous. He says that "... the wind presses more strongly on the slopes of the waves facing it than on the sheltered side, and it is the tendency of the waves to grow is just able to overcome the viscous dissipation that the waves first formed". The pressure and the viscous dissipation are both

computed on the potential flow. Various forms of his theory have appeared. For example, TD wrote his criterion for instability as

$$U_G > \left[\frac{4\mu_L g}{sU_L}\right]^{1/2} \tag{10}$$

where s, the "sheltering" constant, is a fitting parameter which "fits" their data with $s = 0.01$. Andritsos, Williams and Hanratty (1989) got a fit for more viscous fluids with $s = 0.06$. Values of s as great as 6 have been used.

Lin and Hanratty (1986) (LH) re-examine the growth of small amplitude long wavelength disturbances. Their approach differs from classical KH linear stability theory in that liquid phase viscous and inertia terms are included. They also take into account shear stresses at the gas–liquid interface and the component of the pressure out of phase with the wave height. They present their theory for channel flow, as well as pipe flow. In this case, their treatment of the pipe geometry is similar to that used by TD. They study two cases, turbulent gas-turbulent liquid and turbulent gas-laminar liquid. For the sake of simplicity we will cite their transition criterion only for horizontal channel flow:

(a) turbulent gas–turbulent liquid

$$j^* > K\alpha^{3/2} \tag{11}$$

with

$$\frac{1}{K^2} = 1 + \left(\frac{\alpha}{1-\alpha}\right)^{0.714}\left(\frac{C_R}{\overline{u}_L} - 1\right)^2\left[1 + (1+\phi)\left(\frac{\alpha}{1-\alpha}\right)\right]^{1.14}\left(\frac{\rho_G}{\rho_L}\right)^{0.143}\left(\frac{f_i}{f_s}\right)^{0.143}\left(\frac{\upsilon_G}{\upsilon_L}\right)^{0.286} \tag{12}$$

where v is the kinematic viscosity and $\phi \cong f_i/f_s$ is the ratio of the interface and surface friction factors. Here $C_R/\overline{u}_L$, and therefore K, is a function of the void fraction α, f_i/f_s, and fluid properties for a fully developed flow. C_R is the real part of the wave velocity C.

(b) turbulent gas–laminar liquid

$$j^* = K_l\alpha^{3/2}, \tag{13}$$

with

$$K_l = \left[1 - \frac{\Omega Z^2}{(1-\alpha)^3}\left(\frac{\upsilon_G^4}{\upsilon_L^2 g B^3}\right)\left(\frac{BU_{SG}}{\upsilon_G}\right)^{3.5}\right]^{1/2} \tag{14}$$

where Ω is a function of $C_R/\overline{u}_L$ and Z is defined as follows:

$$Z = \frac{1}{60.15}\left(\frac{1-\alpha}{\alpha}\right)^2\left[1 + \frac{4}{3}\left(\frac{1-\alpha}{\alpha}\right)\right]\left(\frac{\rho_G}{\rho_L}\right) \tag{15}$$

For large υ_L, $K_l \cong 1$ and the stability condition reduces to (6).

Barnea and Taitel (1993) (BT) perform a long wavelength stability analysis of stratified flow on the two fluid model equations, for round pipes. They take into account shear stresses and interfacial tension (only to obtain a dispersion equation). They use friction factors to evaluate the shear stresses, in the same way as TD, to determine the equilibrium liquid level h_L. In fact, they

follow the same procedure to determine the neutral stability line on a flow chart, including the geometry treatment. The main difference is that they take into account shear stresses not only to compute h_L but also the critical gas velocity U_G. According to their criterion transition from stratified flow occurs when

$$U_G > K\left[(\rho_L R_G + \rho_G R_L)\left(\frac{\rho_L - \rho_G}{\rho_L \rho_G}\right) g \frac{A}{\frac{dA_L}{dh_L}}\right]^{1/2}. \tag{16}$$

Notice that when $\rho_L \gg \rho_G$

$$(\rho_L R_G + \rho_G R_L)\left(\frac{\rho_L - \rho_G}{\rho_L \rho_G}\right) A = \left(\frac{\rho_L - \rho_G}{\rho_G}\right) A_G,$$

and (16) looks almost like (9).

If $K = 1$, Eq. (16) corresponds to what BT call the inviscid KH (IKH) approach. If $K = K_v$, where

$$K_v = \sqrt{1 - \frac{(C_V - C_{IV})^2}{\frac{\rho_L - \rho_G}{\rho} g \frac{A}{dA_L/dh_L}}} \tag{17}$$

then (16) corresponds to their viscous KH (VKH) approach. Here, $\rho = \rho_L/R_L + \rho_G/R_G$ and the term $(C_V - C_{IV})^2$ takes into account the shear stresses. After BT,

> "... as the liquid viscosity increases the contribution of the term in (16) diminishes and for high viscosity both approaches yield almost the same results. The fact that the results obtained by the VKH analysis, which takes into account the shear stresses, are different from those using the IKH approach at low viscosities, while the two approaches yield almost to the same result at high viscosity, is indeed puzzling."

FJ study the stability of stratified gas–liquid flow in a horizontal rectangular channel using VPF. Their analysis lead to an explicit dispersion relation (see Table 1) in which the effect of surface tension and viscosity on the normal stress are not neglected but the effects of shear stresses are neglected. The authors point out that:

> "The effects of surface tension are always important and actually determine the stability limits for the cases in which the volume fraction of gas is not too small. The stability criterion for VPF is expressed by a critical value of the relative velocity."

The neutral curve (3) of FJ gives rise to the surprising result that the viscosity and density ratios

$$\hat{\mu} = \frac{\mu_G}{\mu_L} \quad \text{and} \quad \hat{\rho} = \frac{\rho_G}{\rho_L} \tag{18}$$

play a critical role in KH stability despite the fact even when $\rho_G \ll \rho_L$ and $\mu_G \ll \mu_L$.

When $\hat{\mu} = \hat{\rho}$ =(which can be expressed as $\upsilon_G = \upsilon_L$, where $\upsilon = \mu/\rho$ is the kinematic viscosity) Eq. (18) for marginal stability is identical to the equation for neutral stability of an inviscid fluid, even though $\hat{\mu} = \hat{\rho}$ does not mean that the fluids are inviscid. Moreover, the critical velocity is

Table 1
Dispersion equation for various authors: $A_R\omega^2 + 2(B_R + B_I)\omega + (C_R + 2C_I) = 0$

Coefficient	IKH (with surface tension)	Barnea and Taitel (1993)	VPFHK (2000)
A_R	$\rho_G \coth(kh_G) + \rho_L \coth(kh_L)$	$\rho_G\left(\frac{1}{R_G}\right) + \rho_L\left(\frac{1}{R_L}\right)$	$\rho_G \coth(kh_G) + \rho_L \coth(kh_L)$
B_R	$-k[\rho_g U_G \coth(kh_G) + \rho_L U_L \coth(kh_L)]$	$-k\left[\rho_G U_G\left(\frac{1}{R_G}\right) + \rho_L U_L\left(\frac{1}{R_L}\right)\right]$	$-k^2[\rho_G U_G \coth(kh_G) + \rho_L U_L \coth(kh_L)]$
B_I	0	$\frac{1}{2}\left[\frac{\partial F}{\partial U_L}\left(\frac{1}{R_L}\right) - \frac{\partial F}{\partial U_G}\left(\frac{1}{R_G}\right)\right]$	$k[\mu_G \coth(kh_G) + \mu_L \coth(kh_L)]$
C_R	$-k(\rho_L - \rho_G)g + k^2[\rho_G U_G^2 \coth(kh_G) + \rho_L U_L^2 \coth(kh_L - k^3\gamma)]$	$-k^2(\rho_L - \rho_G)g\left(\frac{A}{A'_L}\cos\beta\right) + k^2\left[\rho_G U_G^2\left(\frac{1}{R_G}\right) + \rho_L U_L^2\left(\frac{1}{R_L}\right)\right] - k^4\gamma\left(\frac{A}{A'_L}\right)$	$-k(\rho_L - \rho_G)g + k^2[\rho_G U_G^2 \coth(kh_G) + \rho_L U_L^2 \coth(kh_L - k^3\gamma)]$
C_I	0	$k\frac{1}{2}\left[\frac{\partial F}{\partial U_L}U_L\left(\frac{1}{R_L}\right) - \frac{\partial F}{\partial U_G}U_G\left(\frac{1}{R_G}\right) - \frac{\partial F}{\partial h_L}\left(\frac{1}{A'_L}\right)\right]$	$-k^3[\mu_G U_G \coth(kh_G) + \mu_L U_L \coth(kh_L)]$

Here $F = \frac{\tau_G S_G}{A_G} - \frac{\tau_L S_L}{A_L} + \tau_i S_i\left(\frac{1}{A_G} + \frac{1}{A_L}\right) - (\rho_L - \rho_G)g\sin\beta$, where $\tau_G = f_G\frac{\rho_G U_G^2}{2}$, $\tau_L = f_L\frac{\rho_L U_L^2}{2}$, and $\tau_i = f_i\frac{\rho_i(U_G - U_L)^2}{2}$.
Furthermore, $F = F[U_G, U_L, h_L] = F[U_{SG}(U_G, h_L), U_{SL}(U_L, h_L), h_L]$. Note $U_{SG} = U_G R_G$ and $U_{SL} = U_L R_L$.

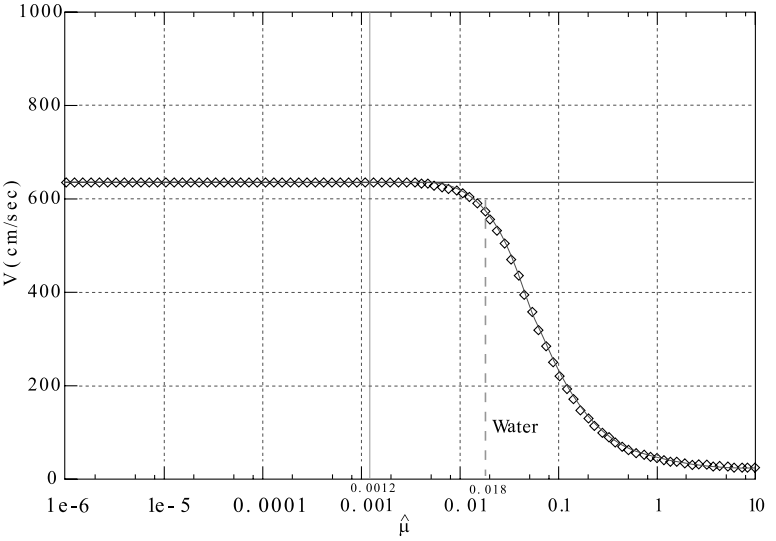

Fig. 1. After Funada and Joseph (2001). Critical velocity $V = |U_G - U_L|$ vs. $\hat{\mu}$ for $\alpha = 0.5$. The critical velocity is the minimum value on the neutral curve. The vertical line is $\hat{\mu} = \hat{\rho} = 0.0012$ and the horizontal line at $V = 635.9$ cm/s (6.359 m/s), the critical value for inviscid fluids. The vertical dashed line at $\hat{\mu} = 0.018$ is for air and water.

maximum at $\hat{\mu} = \hat{\rho}$; hence the critical velocity is smaller for *all* viscous fluids such that $\hat{\mu} \neq \hat{\rho}$ and is smaller than the critical velocity for inviscid fluids. All this is well explained by the authors with their Fig. 4 (which we reproduce here in Fig. 1). Fig. 1 shows that $\hat{\mu} = \hat{\rho}$ is a distinguished value that can be said to divide high viscosity liquids with $\hat{\mu} > \hat{\rho}$ from low viscosity liquids with $\hat{\mu} < \hat{\rho}$. As a practical matter the stability limit of high viscosity liquids can hardly be distinguished from others, while the critical velocity decreases sharply for low viscosity fluids.

The condition $\hat{\mu} = \hat{\rho}$, may be written as

$$\mu_L = \mu_G \frac{\rho_L}{\rho_G} \tag{19}$$

For air and water

$$\mu_L = 0.015 \text{ Pa s} \tag{20}$$

Hence $\mu_L < 0.015$ Pa s is low viscosity liquid provided that $\rho_L \approx 1000$ kg/m^3.

3.1. Dispersion equations

Table 1 presents the coefficients of complex growth rate ω of the dispersion equation obtained corresponding to the classical KH analysis, as well as to BT's and FJ's, from which they develop their stability criteria.

The dispersion equation can be written as

$$A_R\omega^2 + 2(B_R + B_I)\omega + (C_R + 2C_I) = 0$$

where $\omega = kC$, and the subscripts R and I stand for real and imaginary part.

BT make some simplifications by using the derivative with respect to the superficial gas and liquid velocities, U_{SG} and U_{SL} rather than with respect U_G and U_L. Therefore, B_I and C_I in Table 1 reduce to

$$B_I = \frac{1}{2}\left[\left.\frac{\partial F}{\partial U_{SL}}\right|_{U_{SL},h_L} - \left.\frac{\partial F}{\partial U_{SG}}\right|_{U_{SL},h_L}\right] \quad \text{and} \quad C_I = -k\frac{1}{2}\left.\frac{\partial F}{\partial R_L}\right|_{U_{SG},U_{SL}},$$

respectively. Here F is the sum of the acting forces in the combined momentum equation of the two fluid model. After BT's nomenclature, R denotes the phase holdup.

In Table 1 we can see that the coefficient A_R for the three models can be written as

$$A_R = \rho_G a_{R1} + \rho_L a_{R2}. \tag{21}$$

where a_{R1} and a_{R2} are function of the geometry only.

Similarly, for the coefficient B_R, or

$$B_R = -k[(\rho_G U_G)b_{R1} + (\rho_L U_L)b_{R2}]. \tag{22}$$

Again, b_{R1} and b_{R2} are function of the geometry only. Notice that the power of k is 1 for each model. Now, if we write the coefficient C_R as follows:

$$C_R = -k(\rho_L - \rho_G)g c_{Rk1} + k^2[(\rho_G U_G^2)c_{Rk2,1} + (\rho_L U_L^2)c_{Rk2,2}] - k^3\gamma c_{Rk3}, \tag{23}$$

we find that not all the $c_{Rkm,n}$ coefficients coincide. Table 2 shows the details.

The coefficient c_{Rk1} corresponds to the term that takes into account the effect of gravity. It is 1 for KH and the FJ model, but different from 1 for the BT model. In this case, geometry plays a role through the term (A/A'_L). But the main difference is due to the presence of k. This raises the

Table 2
Coefficient for C_R

Coefficient	IKH (with surface tension)	Barnea and Taitel (1993)	VPFKH (2001)
c_{Rk1}	1	$k\left(\frac{A}{A'_L}\cos\beta\right)$	1
$c_{Rk2,1}$	$\coth(kh_G)$	$\frac{1}{R_G}$	$\coth(kh_G)$
$c_{Rk2,2}$	$\coth(kh_L)$	$\frac{1}{R_L}$	$\coth(kh_L)$
c_{Rk1}	1	$k\left(\frac{A}{A'_L}\right)$	1

power of k, from 1 to 2, when the complete gravity term of C_R is considered. It is important to recall what is the exact origin of this term. In the KH and FJ cases, it comes from the body forces in the momentum equation. In the BT model, it arises from the treatment of the pressure and not from the body forces. Recall F does include a gravity term, which comes from the body forces.

The coefficients $c_{Rk2,1}$ and $c_{Rk2,2}$ are functions of geometry only.

Finally, the coefficient c_{Rk3} corresponds to the term that takes into account the effect of surface tension. It is 1 for KH and the FJ model, but different from 1 for BT, where k is present. This raises the power of k from 3 to 4 when the complete surface tension term of C_R is considered. In KH and the FJ model, this term has an associated k raised to the third power and it comes directly from the analysis of the surface tension condition. In the BT model the power of k is 4. It arises, though, from a more complex analysis. They develop a combined momentum equation (two fluid model), in which the pressure term has been manipulated as follows. They first assume that the pressure is only hydrostatic, then they introduce the surface tension condition and finally, they express everything in terms of the liquid holdup h_L. Only then, they perturb the resulting equation. In one last step, they differentiate it with respect to x, so they know all the involved terms. By doing this, they raise the order of the derivative associated to the surface tension term, from 3 to 4. This results in a fourth power for k.

We must point out that even though BT consider surface tension in their dispersion equation, they do a long wave analysis in which surface tension is neglected to develop their stability criterion.

4. Relation of experiments to theory

The study of gas–heavy oil flow is best done as an emphasis in a general study of gas–liquid flow in which flow regime transitions, like the transition from stratified to slug flow are targets. The most common correlation used to calculate the conditions for the transition from one flow regime to another is Mandhane plot 24 (Mandhane et al., 1974) shown in our Fig. 2. The Mandhane plots are framed in terms of superficial velocities $U_{SG} = Q_G/A$, $U_{SL} = Q_L/A$, which are related to the mean velocities used in analysis by

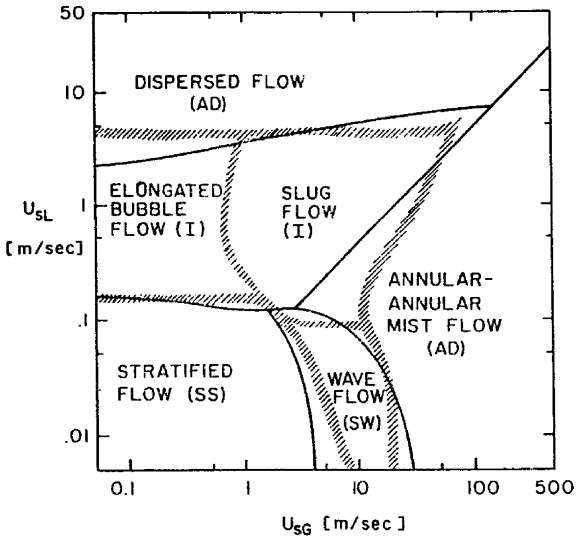

Fig. 2. After Taitel and Dukler (1976). Comparison of theory and experiment. Water–air, 25 °C, 1E + 05 Pa (1 atm), 0.0254 m diameter, horizontal; — theory; ///// Mandhane et al. (1974). Regime descriptions as in Mandhane.

$$U_{SG} = \alpha U_G, \quad U_{SL} = (1-\alpha)U_L \tag{24}$$

Criteria, like those arising from (3) for which the neutral curve is given by

$$V^2 = (U_G - U_L)^2 = f(\alpha) \tag{25}$$

should be expressed in Mandhane diagrams as

$$\left(\frac{U_{SG}}{\alpha} - \frac{U_{SL}}{1-\alpha}\right)^2 = f(\alpha) \tag{26}$$

To plot this kind of criterion it is necessary to know α at (U_{SG}, U_{SL}) point.

LH note that "... the general consensus is that this plot is most reliable for air and water flowing in a small diameter pipe". They get a quite different flow chart even for air and water, when the pipe diameter is larger as shown in Fig. 3.

The Mandhane charts cannot well describe the flow regimes that can arise in all circumstances. The coordinates of the charts are superficial velocities, dimensional quantities that do not reflect any consequence of similarity, Reynolds numbers, Weber numbers, etc. Mandhane charts lack generality since each sheet requires specification of a set of relevant parameters like fluid viscosity, surface tension, pressure level and gas density, turbulence intensity data, pipe radius, gas fraction, etc.

Mandhane charts assume that flow regimes are unique and do not acknowledge the fact that a nonlinear system allows multiple solutions. For example, Wallis and Dobson (1973) have shown that apparently stable slug flow can be initiated by large disturbances in the region where stratified flow is stable (see their section titled "Premature slugging"). Slugs are formed in the 0.0508 m i.d. Intevep flow loop in gas-oil ($\mu_L = 0.480$ Pa s) flows at small liquid velocities. These slugs are

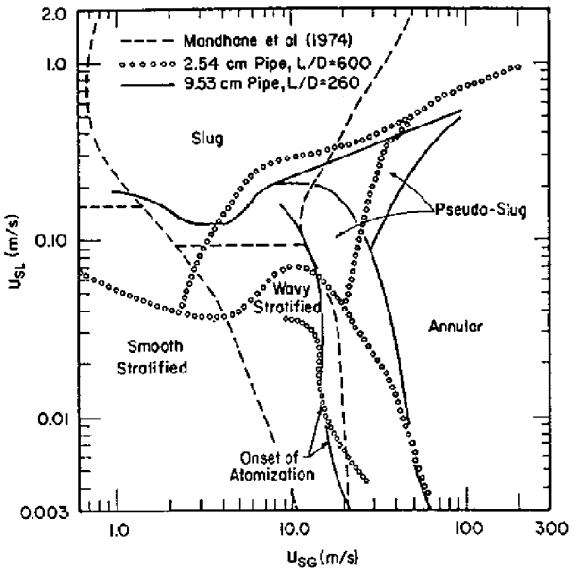

Fig. 3. After Lin and Hanratty (1987). Flow regime map for air and water flowing in horizontal 0.0254 and 0.0953 m pipes. U_{SL} and U_{SG} are superficial velocities related to U_L and U_G by (23).

separated regions of apparently stable stratified flow with a perfectly flat free surface. The length of stable stratified flow between slugs can be nearly the length of the flow loop. This may also be interpreted as "premature" slugging though it is more appropriate to describe it as a multiple solution; slug flow and stratified flow exist at one and the same point on the flow chart.

From the practical point of view, the existence of multiple solutions points to the desirability of a careful analysis of domains of attraction of stable solutions. The appearance of slugs in a region of stable stratified flow points to a careful analysis of the disturbance level at the inlet where large waves may be created. At the end of the paper on waves Crowley et al. (1992) write that

> "When a new slug forms it requires additional pressure drop to accelerate it. This feeds back to the inlet by acoustic waves in the gas (which can travel upstream) and changes the conditions there. This new "disturbance" eventually grows to form a slug and the cycle repeats. The method of characteristics can represent this cycle, but assumptions (or a separate mechanistic analysis) are needed about this inlet behavior."

It is not possible at present to predict the transition of one flow type to another. The dependence of the empirical charting of flows is also incomplete; there is only sparse data on the dependence of flow type on pipe radius, liquid viscosity, pressure level, atomization level, turbulent intensity. Pressure gradients vs. volume flux, holdup of phases and other process control data are not predictable from first principles or from empirical flowcharting.

The linear theory of stability of stratified flow also does not predict the form of the fluid motion that will arise from instability. The theory does predict the wavelength, frequency and growth rate of small growing disturbances. These disturbances may be attracted to a large amplitude solution on a branch of solutions, which is stable when stratified flow is also stable. This may be the case

for subcritical slugs, which arise as "premature slugging". In the supercritical case small amplitude wavy flows are more likely to arise from the instability of stratified flow. The stability limit should separate stable stratified flow from small amplitude wavy flow (see Fig. 8).

In studying the linear theory of instability it is necessary to consider stability to all small disturbances and the restriction to long waves cannot be justified when the maximum growth rate is associated with waves that are not long.

Rigorous analytical approaches to nonlinear effects are often framed in terms of bifurcation theory. To do bifurcation analysis it is necessary to have an accurate description of the flow that bifurcates. Bifurcation analyses of stratified laminar Poiseuille flow of two liquids in channels can be found in the literature but these flows are rather different than the plug flows considered here; they satisfy no-slip conditions at all boundaries and stress continuity conditions at the interfaces. As far as we know this kind of analysis has not been applied to gas–liquid flows possibly because the gas is turbulent even over much of the region where stratified flow is stable.

One value of bifurcation theory is that many of its results are generic so that aspects of nonlinear behavior apply to many different kinds of problems without knowing details of any one. In the usual case the bifurcation of the basic flow occurs at a critical point; in the case of KH instability we lose stability of plug flow when V exceeds the critical value V_c. For $V > V_c$ the basic flow is unstable. Generically a nonlinear solution will bifurcate at criticality; if the nonlinear solution bifurcates with $V > V_c$ it is supercritical and generically stable, if $V < V_c$ it is subcritical and generically unstable. In the case of KH instability, the basic solution is unstable to a time periodic disturbance so that the bifurcating solutions will also be time periodic; this is called a Hopf bifurcation (see Iooss and Joseph, 1990).

It is of interest to speculate how some outstanding experimental observations on the loss of stability of stratified flow may be explained by bifurcation. First, we recall that Wallis and Dobson (1973) reported very robust data on premature slugging, slugs when $V < V_c$. Andritsos and Hanratty (1987) report that stratified flow loses stability to regular waves when the viscosity is small and directly to slugs when the viscosity is large. We too observed what could be interpreted as premature slugging.

Premature waves would be described by subcritical bifurcation as in the diagram of Fig. 4. A supercritical bifurcation to regular waves is shown in Fig. 5. Perhaps there is a change from

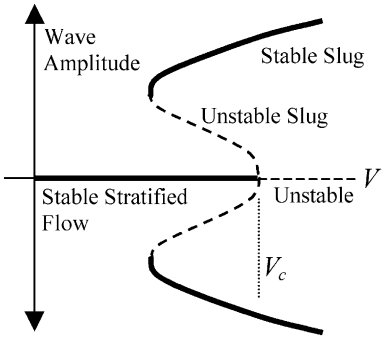

Fig. 4. Bifurcation diagram for premature slugging. When stratified flow loses stability it is attracted through an unstable subcritical branch to a large amplitude stable solution in which the wave amplitude increases with V.

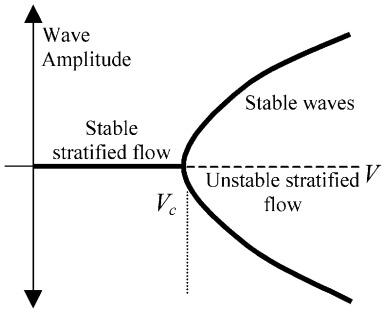

Fig. 5. Bifurcation diagram to explain bifurcation of regular supercritical waves. The stable wave that replaces stratified flow as V is increased may have a very small amplitude, unlike Fig. 4.

supercritical to subcritical bifurcation as the viscosity is increased in the experiments of Andritsos and Hanratty (1987). Many other bifurcation scenarios are possible.

5. Experimental setup

Experiments were carried out in a 0.0508 m i.d. flow loop facility at PDVSA-Intevep. Fig. 6(a) shows the experimental facility diagram, which consist of the following modules:

- handling and measuring for the liquid phase,
- handling and measuring for the gas phase,
- test section,
- non-conventional separation.

In the facility a maximum flow rate of liquid around 1.11E−02 m^3/s and 3.89E−01 sm^3/s for compressed air at 8.62E+05 Pa (125 Psig) can be handled. The liquid (lube oil, 0.480 Pa s) is pumped using a gear pump with a variable speed control. The flow rate of liquid is measured with a flow meter (Micromotion). The air is supplied using two compressors. The flow rate is controlled by three flow control valves and measured with an orifice plate and/or a vortex meter. Air is injected in a "T" injection point where gas and oil are mixed (see Fig. 6(b)). The total length of the test section is 64 m and is conformed by 42 m for flow region development; 17.70 m of transparent acrylic pipe, equipped with transmitters for: pressure, temperature, differential pressure and a high-speed video camera. Differential pressure transducers are used to measure the pressure drop between pressure taps. After the test section, the oil–air mixture is separated in a non-conventional separator. Afterwards, the liquid returns to the tank and the air is vented to the atmosphere.

Air was not always injected at a "T" injection. At the beginning of the experiments a "Y" injection point was used (see Fig. 6(b)). This configuration allowed a rather chaotic mixing process. We avoided that with a new design, which allows the gas and liquid to contact each other in a sort of stratified configuration, as shown in Fig. 6(b). This, we think, avoids entrance perturbations, which could promote premature slugging.

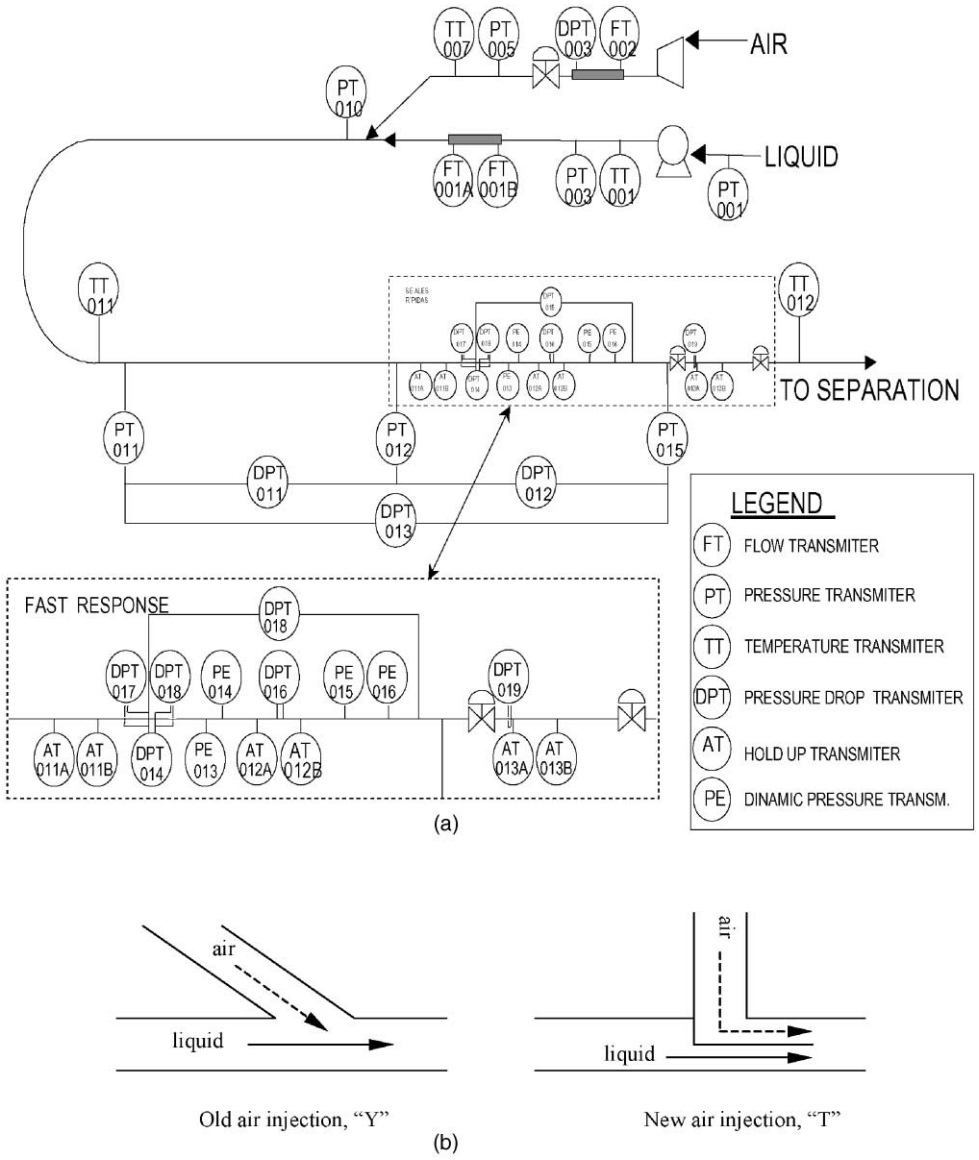

Fig. 6. Experimental setup: (a) PDVSA-Intevep 0.0508 m i.d. flow loop and (b) details of the gas injection point.

6. Results

In this section we will present and compare against theory data from literature for air–water flow in channels and data obtained at the PDVSA-Intevep 0.0508 m i.d. flow loop for air–oil ($\mu_L = 0.480$ Pa s) flow.

6.1. Gas–liquid flow in channels

Plots of $j^* = U_G\alpha\sqrt{\rho_G}/\sqrt{gH(\rho_L - \rho_G)}$ vs. void fraction α together with the slug flow experimental values for air–water flow of Wallis and Dobson (1973), and Kordyban and Ranov (1970) are shown in Fig. 7. Here (a) shows plain linear theories such as long wave IKH, long wave VKH from LH and all waves VPFKH from FJ. Fig. 7(b) shows heuristic adjustments of theories in (a), obtained by multiplying the critical j^* by α.

It is widely acknowledged that nonlinear effects at play in the transition from stratified to slug flow are not well understood. The well-known criteria of TD, based on a heuristic adjustment of the linear inviscid long wave theory for nonlinear effects, is possibly the most accurate predictor of experiments. Their criterion replaces $j^* = \alpha^{3/2}$ with $j^* = \alpha^{5/2}$. We obtain the same heuristic adjustment for nonlinear effects on FJ's VPFKH, as well as LH's approach, by multiplying the critical value of velocity in Fig. 7(a) by α, as shown in Fig. 7(b). Models in (a) that would

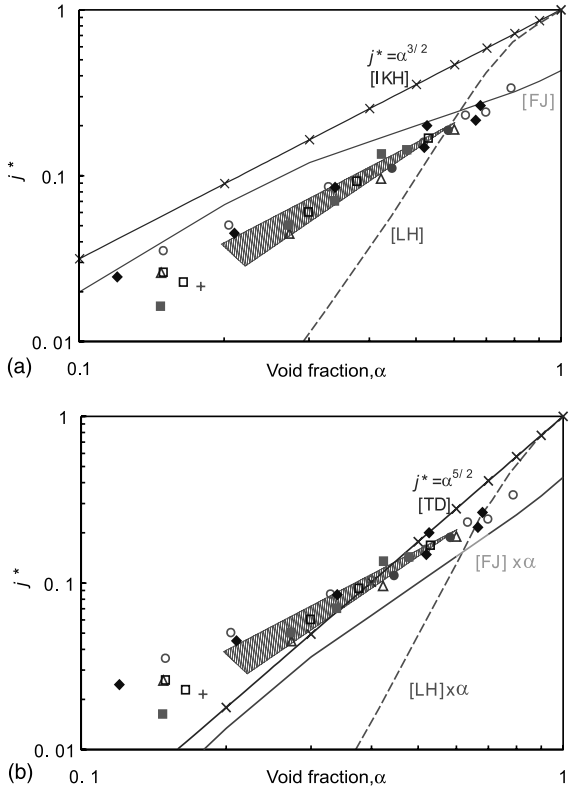

Fig. 7. j^* vs. α. Comparison of theory and experiments in air–water channel flow. All the data points are slug data points by Wallis and Dobson (1973). The shaded region is from experiments by Kordyban and Ranov (1970). (a) Linear theories, including $j^* = \alpha^{3/2}$, which is the long wave criterion for IKH, FJ and LH. (b) Nonlinear effects. Heuristic adjustments of theories in (a), obtained by multiplying the critical j^* by α. Notice that $j^* = \alpha^{5/2}$ is TD model.

under-predict the data predict it very well in (b). On the other hand, the heuristic adjustment for nonlinearity does not make a great change in the results of LH, shown in Fig. 7.

6.2. Gas–liquid flow in a 0.0508 m i.d. pipeline

Fig. 8 presents a Mandhane flow chart for PDVSA-Intevep data from a 0.0508 m i.d. flow loop for air–oil ($\mu_L = 0.480$ Pa s) flow. The identified flow patterns are SS, wavy stratified (SW), slug (SL) and annular (AN). The neutral stability criteria for stratified flow after the following authors are also presented; [J]: –, TD: stars, BT: +, IKH: ×, FJ: broken line, FJ multiplied by α or FJ × α: heavy line.

To evaluate all the criteria, liquid equilibrium level h_L was first computed following the TD procedure, which is described in Section 2. This is done in order to get the void fraction α, and hence the liquid and gas superficial velocities U_{SL} and U_{SG}, respectively. This is consistent with [J] and BT's VKH and IKH criteria. However, the IKH stability criterion was evaluated in a new way; we used the condition $\hat{\mu} = \hat{\rho}$, which FJ describe as "a distinguished value that can be said to divide high viscosity liquids with $\hat{\mu} < \hat{\rho}$ from low viscosity liquids". Since TD's procedure to compute h_L involves viscosity effects, we thought that using the $\hat{\mu} = \hat{\rho}$, which gives $\mu_L = 0.015$ Pa s for the studied system, is more coherent with an "inviscid" criterion than using the actual liquid viscosity $\mu_L = 0.481$ Pa s. The $\hat{\mu} = \hat{\rho}$ condition was also used with the FJ and FJ × α criteria.

Fig. 8 shows that a few stable (open circles) points are above the TD neutral stability curve (stars). It also shows that some unstable or (SW) points (open squares) are to the right of the BT neutral stability curve (+), which is higher and above some (SL) experimental points (solid triangles). The IKH neutral curve (×) is way above the TD and BT curves. It includes in the predicted stable region most of the (SL) and (AN) experimental points (triangles and diamonds),

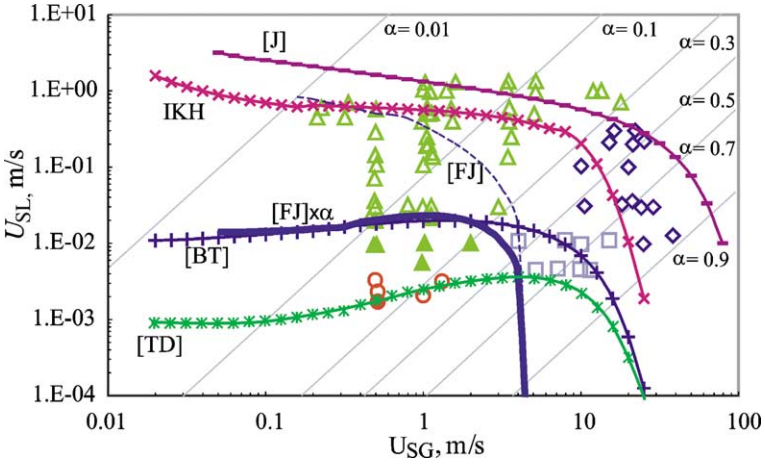

Fig. 8. Mandhane flow chart for PDVSA-Intevep data from 0.508 m i.d. flow loop with air and 0.480 Pa s lube oil. The identified flow patterns are SS (open circles), SW (open square), SL (triangles) and AN (open diamonds). Stratified to non-stratified flow transition theories after different authors are compared; [J]: –, TD: stars, BT: +, IKH with $\hat{\mu} = \hat{\rho}$ IKH: ×, FJ: broken line, Funada and Joseph multiplied by α (2001) FJ × α: heavy line. Constant void fraction α lines are indicated. Notice that the curves FJ and FJ × α sharply drop around $U_{SG} \cong 5$ m/s.

respectively. Same thing happens with the [J] neutral stability curve (–). Evidently both [J] and IKH criteria fail to predict the instability threshold for the studied system. The [FJ] neutral stability curve (broken line) is very close to the IKH one for $U_{SG} < 1$ m/s, but drops sharply around $U_{SG} \cong 5$ m/s. However, the FJ $\times$ α (heavy line) overlaps the BT one, dropping sharply around $U_{SG} \cong 5$ m/s. The FJ $\times$ α stability curve was obtained multiplying $\hat{V}_c(\hat{k}_c)$ by α, which is the TD "heuristic adjustment for nonlinear effects".

Both FJ neutral curves (broken and heavy lines) illustrate two interesting issues: First, the sharp dropping around $U_{SG} \cong 5$ m/s. Second, they both successfully predict the instability threshold; all the (SW) experimental data points (open square), which are unstable, are outside the predicted stable region.

The $U_{SG} \cong 5$ m/s limit surprisingly coincides with LH's experimental observations in a 0.0508 m i.d. pipeline with a water–air system. They found that

> "... Transitions from stratified to slug flow for a superficial gas velocity $U_{SG} < 5$ m/s were observed for flows that were not fully developed; i.e. the liquid was caused to flow through the pipe by hydraulic gradients, as well as the drag of the gas at the interface. For $U_{SG} > 5$ m/s the transition to slug flow occurred for a stratified layer that had irregular large-amplitude KH waves on it. The increase in the superficial liquid velocity U_{SL}, required to initiate slugging when U_{SG} is increased beyond $U_{SG} = 5$ m/s, can be explained by the presence of KH waves which cause an increase in the drag and an associated large decrease in h_L (Andritsos et al., 1989)."

Our experimental data also shows the $U_{SG} \cong 5$ m/s limit. To the right of both FJ curves ($U_{SG} > 5$ m/s), and at low superficial liquid velocities ($U_{SL} < 0.01$ m/s), there are unstable or (SW) data points (open squares). This result agrees with the idea of KH theory, which predicts the instability of an interface, and not necessarily the transition to slug flow (SL, triangles). Another agreement with LH experimental observations is "... the increase in the superficial liquid velocity, U_{SL}, required to initiate slugging when U_{SG} is increased beyond $U_{SG} = 5$ m/s ..." which they explain by the presence of KH waves and which cause an increase in the drag and an associated large decrease in h_L.

Fig. 8, like Fig. 7, shows that the FJ basic linear approach does not account for nonlinear effects or "premature" slugging. In Fig. 8, below the FJ broken line, one finds most of the (SL, triangles) experimental points. However, when FJ critical velocity is multiplied by the TD heuristic correction factor α most of the (SL, triangles) points are above the new curve (the heavy line identified as FJ $\times$ α in Fig. 8). Those (SL) points below the heavy line (solid triangles) can be interpreted as genuine "premature" slugs, and the result of bifurcation of stability. Moreover, all those points were obtained before the gas injection configuration was changed from "Y" to "T" (see Fig. 6(b)). The stable points (SS, open circle) were obtained after the injection device was changed and experiments continued. The stable (SS) point, the only solid circle in Fig. 8, was obtained with the "T" injection point. However, we must point out that a single liquid slug was observed one hour and a half after the (U_{SG}, U_{SL}) condition was set. This test lasted 5 h total, and after that single slug no more slugs were observed. After this experiment we checked the flow loop level and found out inclination angles up to $O(10^{-2})$ degrees. Once the flow loop was leveled, the other (SS) experimental points were obtained, for which not a single slug was observed. This result

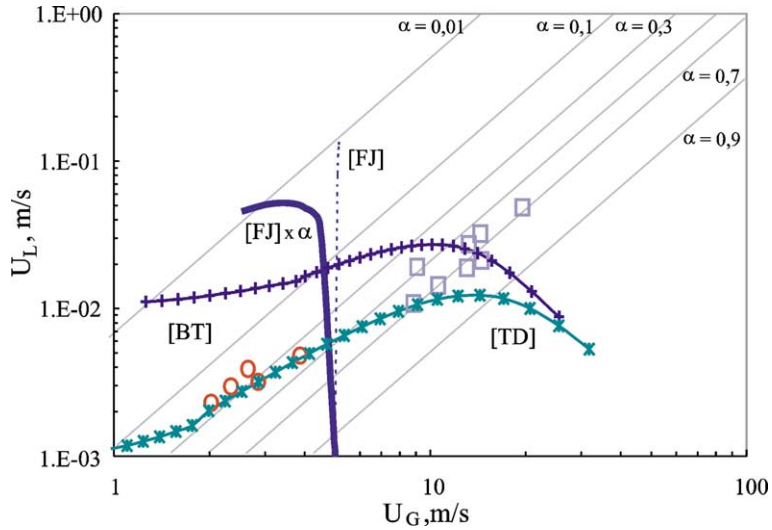

Fig. 9. Local liquid velocity U_L vs. local gas velocity U_G for PDVSA-Intevep data from 0.508 m i.d. flow loop with air and 0.480 Pa s lube oil (same as in Fig. 8). The identified flow patterns are SS (open circles), SW (open squares). Stratified to non-stratified flow transition theories after different authors are compared; TD: stars, BT: +, FJ: broken line, Funada and Joseph multiplied by α (2001) FJ $\times$ α: heavy line. Constant void fraction α lines are indicated. Notice that the curves FJ and FJ $\times$ α sharply drop around $U_G \cong 5$ m/s, separating SS data from SW data.

suggests that another source of "premature" slugs could have been liquid accumulation at some points in the flow loop.

Fig. 9 compares theory and experiments in the average velocity rather than superficial velocity plane. Here stable (SS, circles) and unstable (SW, squares) data points were obtained with our 0.0508 m i.d. flow loop for air–oil ($\mu_L = 0.480$ Pa s) flow. The neutral stability criteria for stratified flow after the following authors are also presented; TD: stars, BT: +, FJ: broken line, FJ multiplied by α or FJ $\times$ α: heavy line. The linear FJ and heuristic nonlinear FJ $\times$ α criteria separate stable stratified flow from SW flow.

7. Concluding remarks

1. In this paper we compare results from different theories of the KH instability of stratified gas–liquid flow with each other, to old data for water–air and to new data, presented here, on heavy oil (0.480 Pa s).
2. The theories discussed are due to [J], TD, LH, BT and FJ. The computations for heavy oil for these theories are done in this paper. The comparison of different theories with each other and the comparison of all theories against data—new and old—has not been done before.
3. The theories make different assumptions and the predicted stability limits differ widely (see Figs. 7–9).
4. TD, LH and BT carry out analysis for instability to long waves without demonstrating that short waves lead to the lowest critical value of instability. FJ study the KH instability to all waves and show that the critical wave is not long and is determined by surface tension.

5. BT give a two-fluid model for the KH instability in which surface tension is included, but they calculate only for long waves for which surface tension plays no role. In the BT theory the surface tension term is proportional to k^4, whereas in the classical theory and other two fluid models it is proportional to k^3.
6. In TD and BT, boundary conditions are not explicitly enforced on the wall and different geometries are recognized by specifying the value of the ratio of the area occupied by the gas A_G to the rate of change of A_L (area occupied by the liquid) with respect to the liquid holdup h_L. No demonstration of the equivalence of these different geometries is given and it is possibly not true.
7. TD and FJ neglect the shear stress; LH and BT include them by way of empirical correlations, which may be chosen to fit data.
8. The viscous normal stress is neglected by TD, LH and BT, whereas it is considered by FJ.
9. FJ carried out analysis using VPF, which predicted that the critical velocity for KH instability is largely independent of viscosity for large kinematic viscosity $v_L > v_G$, but depends strongly on viscosity when $v_L < v_G$. When $v_L = v_G$ the critical velocity is high and equal to that given by VPF.
10. TD and BT, in their IKH analysis, neglect viscosity in the stability analysis but need viscosity for the liquid holdup calculation. When we evaluated the IKH theory, we chose $v_L = v_G$ which gives a liquid viscosity μ_L most consistent with an inviscid analysis.
11. TD constructed a heuristic theory to account for nonlinearity. This theory leads to the multiplication of critical velocity by the gas fraction α and it is widely considered to give the best agreement with observed water–air data. We show that the same argument applied to FJ leads to a slightly better agreement in both the water–air and oil–air cases.
12. Both of the FJ neutral curves (linear and with TD heuristic correction for nonlinear) show a sharp dropping around $U_{SG} \cong 5$ m/s, and leave outside the SW data points and account for nonlinear effects. The$U_{SG} \cong 5$ m/s limit surprisingly coincides with LH experimental observations in a 0.0508 m i.d. pipeline with a water–air system.
13. Our new experimental data on heavy oils also respects the $U_{SG} \cong 5$ m/s limit. This result agrees with the idea that KH theory predicts the instability of an interface, and not necessarily the transition to slug flow.
14. Another agreement with LH experimental observations is the increase in the superficial liquid velocity, U_{SL}, required to initiate slugging when U_{SG} is increased beyond $U_{SG} = 5$ m/s.
15. Recognizing that the TD argument is rather primitive, we explored some ideas about bifurcation theory emphasizing the big difference between subcritical and supercritical bifurcation, but no calculations are given. The case of "premature" slugging identified by Wallis and Dobson (1973), and in the oil–air experiments reported here, explains a subcritical bifurcation.

Acknowledgements

We are thankful to M. Ahow, R. Cabello, J. Colmenares, I. Damia, P. Gonzalez, P. Ortega and A. Pereira, for collecting and processing the data at our flow loop. We are also thankful to T. Funada for computing the critical velocities for the air–lube oil system. This work was supported by PDVSA-Intevep. D.D. Joseph's contribution was also supported by the National Science

Foundation DOE award number CTS-0076648 and by the Army Research Office DA/DAAG55-98-1034.

References

Andritsos, N., Hanratty, T.J., 1987. Interfacial instabilities for horizontal gas–liquid flow in pipelines. Int. J. Multiphase Flow 13, 583–603.

Andritsos, N., Williams, L., Hanratty, T.J., 1989. Effect of liquid viscosity on stratified/slug transitions in horizontal pipe flow. Int. J. Multiphase Flow 15, 877–892.

Barnea, D., 1991. On the effect of viscosity on stability of stratified gas–liquid flow—Aplication to flow pattern transition at various pipe inclinations. Chem. Eng. Sci. 46, 2123–2131.

Barnea, D., Taitel, Y., 1993. Kelvin–Helmholtz stability criteria for stratified flow: viscous versus non-viscous (inviscid) approaches. Int. J. Multiphase Flow 19, 639–649.

Crowley, C.J., Wallis, G.-H, Barry, J.J, 1992. Validation of one-dimensional wave model for the stratified-to-slug flow regime transition, with consequences for wave growth and slug frequency. Int. J. Multiphase Flow 18, 249–271.

Chokshi, R., Schmith, Z., Doty, D., 1996. Experimental studies and the development of a mechanistic model for two-phase flow through vertical tubing, SPE 35676. Western Regional Meeting, Alaska, pp. 255–267.

Jeffreys, H., 1925. On the formation of water waves by wind. Proc. Royal Soc. A 107, 189.

Jeffreys, H., 1926. On the formation of water waves by wind (second paper). Proc. Royal Soc. A 110, 241.

Funada, T., Joseph, D.D., 2001. Viscous potential flow analysis of Kelvin–Helmholtz instability in a channel. Int. J. Multiphase Flow 445, 263–283.

Gómez, L., Shoham, O., Schmith, Z., Chokshi, R., Brown, A., Northhug, T., 1999. A unified model for steady two-phase flow in wellbores and pipelines, SPE 56520, SPE Annual Technical Conference and Exhibition, Houston, Texas, pp. 307–320.

Iooss, G., Joseph, D.D., 1990. Elementary Stability and Bifurcation Theory, second ed. Springer, Berlin.

Joseph, D.D., Liao, T.Y., 1994. Potential flow of viscous and viscoelastic fluids. J. Fluid Mech. 265, 1–23.

Joseph, D.D., Belanger, J., Beavers, G.S., 1999. Breakup of a liquid drop suddenly exposed to a high-speed airstream. Int. J. Multiphase Flow 25, 1263–1303.

Kordyban, E.S., Ranov, T., 1970. Mechanism of slug formation in horizontal two-phase flow. Trans. ASME J. Basic Eng. 92, 857–864.

Lin, P.Y., Hanratty, T.J., 1986. Prediction of the initiation of slugs with linear stability criterion. Int. J. Multiphase Flow 12, 79–98.

Lin, P.Y., Hanratty, T.J., 1987. Effect of pipe diameter on flow patterns for air–water flow in horizontal pipes. Int. J. Multiphase Flow 13, 549–563.

Mandhane, J.M., Gregory, G.A., Aziz, K., 1974. A flow pattern map for gas–liquid flow in horizontal pipes. Int. J. Multiphase Flow 1, 537–551.

Taitel, Y., Dukler, A.E., 1976. A model for predicting flow regimen transitions in horizontal and near horizontal gas liquid flow. AIChE J. 22, 47–55.

Wallis, G.B., Dobson, J.E., 1973. Prediction of the initiation of slugs with linear stability criterion. Int. J. Multiphase Flow 1, 173–193.